Spectroscopic Characterization of the Artificial Siderophore Pyridinochelin

Michael U. Kumke[a,*], Carsten Dosche[b], Roman Flehr[a],
Wolfram Trowitzsch-Kienast[c], and Hans-Gerd Löhmannsröben[a]

[a] Institute of Chemistry, University of Potsdam, Karl-Liebknecht-Str. 24–25, D-14476 Potsdam-Golm, Germany. E-mail: Kumke@chem.uni-potsdam.de
[b] Institute of Physics, University of Potsdam, Am Neuen Palais 10, D-14469 Potsdam, Germany
[c] Technische Fachhochschule Berlin, FB II, Luxemburger Str. 10, D-13353 Berlin, Germany

* Author for correspondence and reprint requests

Z. Naturforsch. **61c**, 741–748 (2006); received June 12/July 14, 2006

Siderophores play a very important role in the uptake process of iron by bacteria. Due to the so-called active transport the uptake of siderophores by bacteria is very specific, which makes the use of siderophores as effective shuttles for antibiotics in the treatment of infections and other diseases caused by bacteria highly attractive. In order to further investigate the transport and incorporation of siderophores into the bacteria cells, distinct molecular probes are needed. Especially artificial siderophores, that show a specific intrinsic fluorescence, are highly attractive for such monitoring purposes. A promising candidate of such a fluorescent artificial siderophore is bis-2,3-dihydroxybenzoyl-2,6-dimethylamino-pyridine (pyridinochelin, PY).

The fluorescence properties of PY were investigated in different solvents and in the presence of different metal ions. It was found that PY in its free form shows a complex fluorescence behavior. In methanol a clear dual fluorescence is observed. In aqueous solution intermolecular interactions with water molecules are determining the intrinsic fluorescence. Upon complexation with metal ions (Me^{3+} = Eu^{3+}, Tb^{3+}, Al^{3+}, Fe^{3+}) the fluorescence characteristics changed. The fluorescence quantum yield of PY decreased upon addition of Me^{3+} – except for Al^{3+}, which showed no fluorescence quenching. The fluorescence decay of PY loaded with metal ions showed a nicely mono-exponential fluorescence decay, which was in contrast to PY in the absence of metal ions. This drastic change in the fluorescence properties of PY upon metal ion complexation makes PY highly attractive as a fluorescence probe for the investigation of siderophore action and siderophore-mediated transport processes.

Key words: Siderophores, Fluorescence, Excited State Reactions

Introduction

Siderophores are molecules designed for the specific complexation of metal ions, especially iron. They are produced by bacteria in order to facilitate the transport of Fe^{3+} into the cell. The binding constants for Fe^{3+} are outstandingly high, which enables bacteria to accept Fe^{3+} even under severe environmental conditions. Ligand types of siderophores frequently encountered are catecholate or hydroxamate units (Budzikiewicz 2004; Adolphs *et al.*, 1996). A very important group of siderophores are the pyoverdins, which exhibit an intrinsic fluorescence due to the presence of a dihydroxyquinoline moiety (Bultreys *et al.*, 2004; Ruangviriyachai *et al.* 2004; Barelmann *et al.*, 1996; Budzikiewicz, 1997). The siderophore-Fe^{3+} complexes are taken up by bacteria *via* membrane receptors, so-called iromps (iron induced outer membrane proteins). The highly specific uptake of siderophores by bacteria makes this class of compounds attractive as a shuttle for the transport of antibiotics into bacteria. The combination with antibiotics would allow a highly specific targeting with increased concentrations of antibiotics at the site of action. Moreover, siderophores are also interesting for other medical applications, *e.g.*, in case of an overdose of iron or alumina (Meyer and Trowitzsch-Kienast, 2004; Santos, 2002; Rubini *et al.*, 2002). Since Fe^{3+} (and hence its availability) is an important growth factor, the *in situ* detection of Fe^{3+} at trace levels is very interesting for investigations of the stability and of the dynamics of aquatic ecosystems. Therefore, the development of sensitive and selective sensors for Fe^{3+} is needed. With respect to analytical techniques fluorescence methods are among the most powerful because they perfectly combine sensitivity and selectivity with on-line and *in situ* capabilities. In the investigations of siderophore action attempts have been

0939–5075/2006/0900–0741 $ 06.00

made to use the intrinsic fluorescence of siderophores, to label siderophores with fluorescent dyes, and to use artificial siderophores with fluorescence probes (Namiranian *et al.*, 1997; del Olmo *et al.*, 2003; Bodenant and Fages, 1995; Planche *et al.*, 1999; Fages, 1997; Sohna and Fages, 1997). Fluorescence quenching, formation of excimers, and lanthanide-based energy transfer has been utilized as detection principle to monitor the binding of various metal ions to artificial siderophores.

In order to combine the specific properties of siderophores with those of pharmaceutical compounds, the design of novel, artificial siderophores is of great importance and in a biomimetic approach the well-characterized enterobactin was used as a model (Albrecht-Gary *et al.*, 1996; Meyer and Trowitzsch-Kienast, 1997, 2004; Meyer *et al.*, 2001). Enterobactin binds Fe^{3+} with an extremely high binding constant [*e.g.*, $\log \beta_f \approx 49$ (Meyer and Trowitzsch-Kienast, 2004)] and has been used as model compound for the design of novel siderophore-based compounds before (Meyer and Trowitzsch-Kienast, 2004; Ecker *et al.*, 1988; Tor *et al.*, 1992). Based on computational results bis-2,3-dihydroxybenzoyl-2,6-dimethylamino-pyridine [pyridinochelin (PY), see Fig. 1] was synthesized and tested in feed experiments with different bacteria. It could be shown that the activity of PY was comparable to that of the natural siderophore enterobactin (Meyer *et al.*, 2001).

For investigations of siderophore action in biological systems the application of fluorescent siderophores as *in situ* probes is very attractive. PY shows an intrinsic fluorescence. Based on the structure of PY the presence of intra- and intermolecular H-bonds has to be considered. It is well-known that the formation of H-bonds can have strong effects on the geometric, electronic, and vibrational properties of a compound. Changes in the formation of H-bonds in its ground and electronically excited state can drastically alter the fluorescence properties of a molecule. Hence, in order to use PY as fluorescence probe for the investigation of siderophore action, the basic fluorescence properties of PY with special attention to the presence of excited state intramolecular proton transfer reactions (ESIPT) have to be evaluated. In the aqueous environment also the participation of solvent-assisted intermolecular proton transfer reactions has to be taken into account.

Experimental

The synthesis of bis-2,3-dihydroxybenzoyl-2,6-dimethylamino-pyridine (PY) was described previously (Meyer *et al.*, 2001). The spectroscopic experiments were carried out in methanol (HPLC grade; Roth, Karlsruhe, Germany) and in deionized water. The pH value was adjusted using freshly prepared buffer solutions. A stock solution in the corresponding solvent was prepared and the final concentration was adjusted to $4 \cdot 10^{-5}$ M by dilution with pure solvent.

The measurements were performed in quartz cuvettes (Hellma, Mülheim, Germany) with 1 cm optical pathlength. In the absorption spectroscopy experiments a Cary 500 spectrometer (Varian,

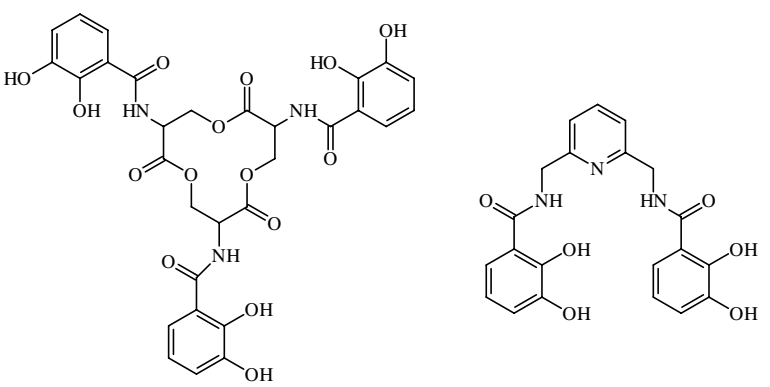

Enterobactin Pyridinochelin

Fig. 1. Structures of enterobactin and pyridinochelin (PY).

Darmstadt, Germany) was used. The stationary fluorescence spectra were recorded on a Fluoromax 3P spectrofluorometer (Yobin Yvon, München, Germany). If not otherwise stated, the excitation wavelength in the steady-state experiments was set to λ_{ex} = 320 nm. The fluorescence quantum yield of PY was determined in methanol using anthracene as a reference [Φ_F = 0.36 (Berlmann, 1971)]. For the quantum yield determination the optical density of the solutions of PY and of anthracene was adjusted to 0.1 at λ_{ex} = 320 nm. The phosphorescence spectra and the phosphorescence decay time were determined with a Fluoromax 3P spectrofluorometer in the phosphorescence mode. The delay between excitation flash and measurement was set to 0.8 μs and the data acquisition time was set to 10 μs.

The time-resolved emission spectra (TRES) were measured using a box car-based method. The fluorescence decays were also measured at different emission wavelengths by time-correlated single photon counting (TCSPC). In the measurement of the TRES an in-lab built setup was used. For the detection an iCCD camera (Picostar F; LaVision, Göttingen, Germany) combined with a polychromator was employed. The gate time of the iCCD was set to 130 ps and the time delay was varied in steps of 10 ps. In the TCSPC experiments the fluorescence decay was measured using a FLS920 lifetime spectrometer (Edinburgh Instruments, Livingston, UK) equipped with a multichannel plate (Europhoton, Berlin, Germany). A Nd-YAG laser and Ti:sapphire laser system were used as excitation source. In the TRES experiments the fourth harmonic (266 nm) of the Nd-YAG-laser (5021 DNS/DPS; B.M. Industrie, Evry, France) with an excitation pulse width of 30 ps was employed. The frequency tripled output (λ_{ex} = 267 nm) of a Ti:sapphire laser operated at 800 nm was used in the TCSPC experiments. The repetition rate of the Ti:sapphire laser was reduced to 4 MHz using a pulse selector (APE, Berlin, Germany).

Results and Discussion

Basic spectroscopic characterization in methanol

In Fig. 2 the normalized absorption (A), fluorescence (F), fluorescence excitation (FX) and phosphorescence (P) spectra of PY in methanol are shown. The absorption maximum is located at λ_{abs} = 317 nm and the fluorescence maximum is found at λ_{em} = 382 nm. The shape of the fluorescence spectrum is asymmetric with a steep flank at the short wavelength side. The large shift between absorption and emission maximum ($\sim$ 5400 cm^{-1}) strongly suggests a change in the molecular geometry or an alteration of the charge distribution in the molecule, *e.g.*, induced by a proton transfer in the excited state (excited state intra- or intermolecular proton transfer, ESIPT). This is further supported by the fact that the absorption (A) and fluorescence excitation (FX) spectrum are shifted relative to each other by about 10 nm in their maxima. This strongly suggests that the electronic ground state of PY is different from its electronic excited state, otherwise absorption and fluorescence excitation would perfectly overlap. The observed spectral shift between the absorption and emission spectra support this conclusion. In steady-state fluorescence experiments an overall fluorescence quantum efficiency Φ_F of 0.08 ± 0.03 was observed. Since PY is expected to show an ESIPT reaction the term *efficiency* rather than *yield* is used in order to stress that the observed fluorescence possibly arises from different excited state (= different forms of PY).

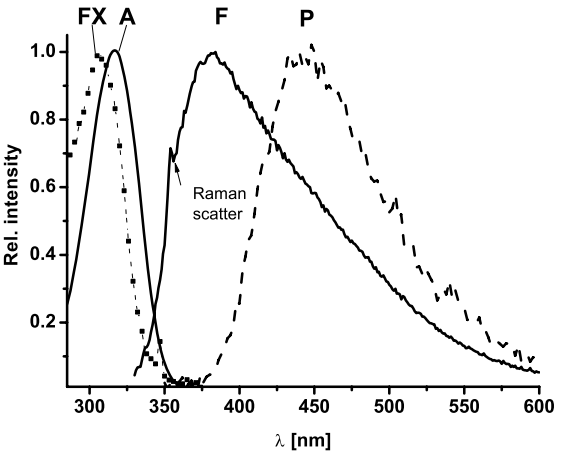

Fig. 2. Absorption (A), fluorescence (F), fluorescence excitation (FX), and phosphorescence (P) spectra of PY in methanol [ε_{315} = 5400 M^{-1} cm^{-1} (Meyer *et al.*, 2001), λ_{ex} = 320 nm]. The absorption and fluorescence spectra were measured at room temperature, while the phosphorescence spectrum was recorded at 77 K.

In Fig. 2 the phosphorescence spectrum of PY in MeOH at 77 K is depicted as well. In comparison to the fluorescence spectrum the maximum of the phosphorescence emission is shifted by about 75 nm relative to the fluorescence maximum to

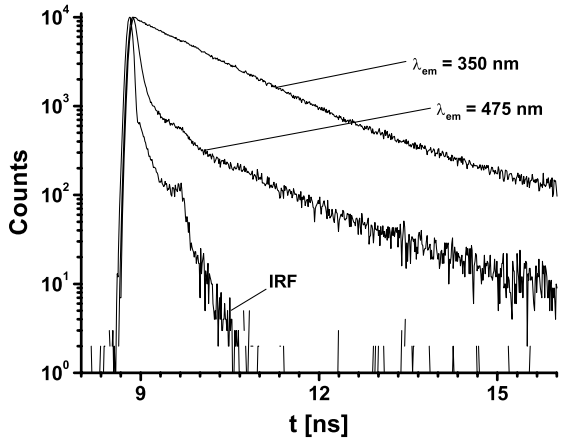

Fig. 3. Fluorescence decays of PY in methanol at λ_{em} = 350 nm and 475 nm, respectively (IRF, instrument response function at λ_{ex} = 266 nm).

450 nm. The phosphorescence decay time was determined to be (10 ± 2) μs.

In time-resolved measurements it was found, that the fluorescence decay of PY was dependent on the emission wavelength λ_{em} and did not follow a single-exponential decay law. In the wavelength range between 360 nm $< \lambda_{em} <$ 500 nm the experimental data were best fitted by a double-exponential decay behaviour. Only at the very edges of the emission spectrum of PY (*e.g.*, at λ_{em} = 350 nm) an almost mono-exponential decay was found. In Fig. 3 the fluorescence decays of PY in methanol at λ_{em} = 350 nm and 475 nm are shown. At λ_{em} = 475 nm a very fast decay component with a decay time $\tau < 100$ ps was determining the fluorescence decay, but a contribution from a second fluorescent component with a longer decay time can clearly be seen. On the other hand, at λ_{em} = 350 nm an almost single-exponential fluorescence decay with a decay time of about τ = 1.2 ns was found. As a general tendency it was observed, that the relative contributions of fast and slow decay components were depending on the emission wavelength. At emission wavelengths > 460 nm the fluorescence decay was dominated by a very fast decay component with a decay time between 50 ps and 100 ps, while at emission wavelengths < 400 nm the major fluorescence decay time was found to be around 1.2 ns (see Table I). Fluorescence excitation spectra with λ_{em} = 375 nm and 475 nm were also recorded. For both detection wavelengths basically the same fluorescence excitation spectra were obtained, which indicates that the different fluorescence emissions originate from the same ground state species.

Table I. Fluorescence decay times (and corresponding relative. amplitudes) of PY in different solvents (λ_{ex} = 266 nm).

Solvent	τ_1 [ps] (%)	τ_2 [ps] (%)
Methanol (λ_{em} = 350 nm)	80 ± 20 (3)	1200 ± 100 (97)
Methanol (λ_{em} = 475 nm)	60 ± 20 (63)	1120 (37)
H_2O (λ_{em} = 375 nm, pH 9)	80 ± 20 (2)	1500 (98)

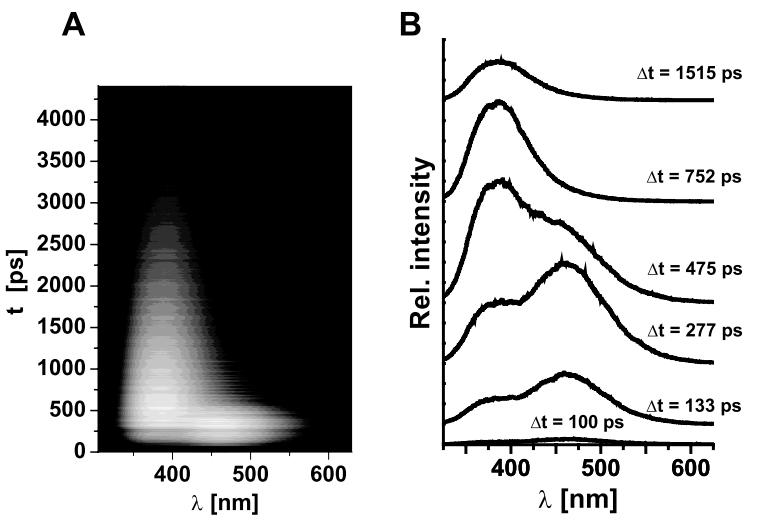

Fig. 4. (A) Time-resolved emission spectrum of PY in methanol (λ_{ex} = 266 nm). (B) Qualitative representation of fluorescence spectra of PY at different times Δt after excitation (λ_{ex} = 266 nm).

In order to further elucidate the fluorescence of PY, time-resolved fluorescence emission spectra (TRES) were measured. Clearly, a dual fluorescence was observed (see Fig. 4). Immediately after excitation a fluorescence component with an emission maximum λ_{em} located around 475 nm was observed and within 200 ps after excitation, a second fluorescence component, which has its maximum around λ_{em} = 375 nm, appeared. A comparison of the decays of the two contributions showed that the fluorescence at 475 nm has vanished completely after ~ 700 ps, while the fluorescence at 375 nm decayed much slower. The TRES results agree perfectly with decay times of 100 ps and 1.2 ns obtained from time-correlated single photon counting (TCSPC) experiments. In the TCSPC experiments the observed fluorescence decays are bi-exponential, because the fluorescence spectra of both components are broad and overlap with each other.

PY in water

We further investigated the absorption and fluorescence of PY in water. In Fig. 5 the absorption spectra of PY in water at pH 1, 7, and 12 are shown. In the absorption spectra for the pH range $1 < pH < 12$ no isosbestic point was observed, which indicates that more than one equilibrium due to protonation and deprotonation reactions might be present. In a factor analysis a number of at least three components was necessary to fit all absorption spectra in the pH range between 1 and 12 satisfactorily. In the inset of Fig. 5 the pH dependencies of the three (operationally defined) species are shown. From the curves two pK_a values were estimated (pK_{a1} = 3.5 and pK_{a2} = 7.2). Considering the chemical structure of PY, it is attractive to assign pK_{a1} to the conjugated base of the pyridine N-group and pK_{a2} to the hydroxy groups of the 1,2-dihydroxybenzene units. It is clear that the second pK_a value is an mean overall value of all hydroxy groups that is not further resolved by our crude approach.

The fluorescence of PY in water was broad and the location of the fluorescence maximum did not change with pH value. The maximum of emission was located at λ_{em} ~ 430 nm. However, the fluorescence intensity was strongly dependent on pH value. While the fluorescence at pH 1 was weak, it increased with increasing pH and showed the strongest fluorescence at pH > 10. The increase of the fluorescence intensity with increasing pH value was not linear. In the range between 4 and 6 only a minor change in fluorescence intensity was observed. It is interesting to note that this pH range corresponds to the pH range in absorption for which the operationally defined intermediate form was assigned (see Fig. 5).

We also measured TRES of PY in water. In contrast to methanol the TRES of PY in water showed no such clear spectrally separated dual fluorescence. The measured decay kinetics were

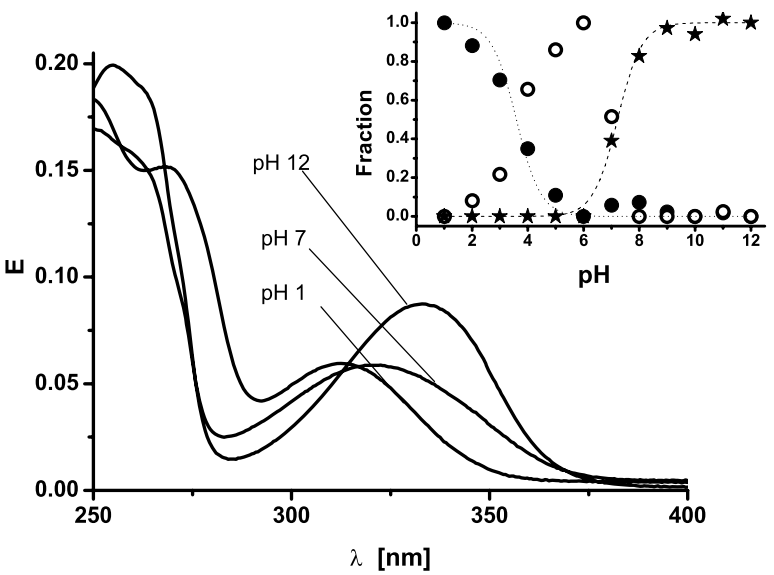

Fig. 5. UV spectra of PY in H_2O at different pH values. Inset: Fractional contribution of assumed three species (● fully protonated, ○ intermediate, and ★ fully deprotonated form of PY) to the overall absorption.

multi-exponential and independent of the detection wavelength.

Complexation of PY with Me^{3+} in methanol

The influence of different metal ions Me^{3+} on the intrinsic fluorescence of PY was determined. In steady-state fluorescence as well as in TRES measurements the influence of Tb^{3+}, Eu^{3+}, Al^{3+}, and Fe^{3+} on the PY fluorescence was further investigated. For Tb^{3+}, Eu^{3+} and Fe^{3+} a strong quenching of the fluorescence intensity was observed.

Upon addition of Me^{3+} the TRES of PY were considerably altered. In methanol the dual fluorescence was reduced with increasing Me^{3+} concentration. Finally, at a ratio of 1:1 between Me^{3+} and PY only one fluorescence component remained. The remaining fluorescence at the 1:1 ratio was very weak. Compared to the uncomplexed form of PY, the maximum of the fluorescence was slightly shifted relative to the short-wavelength component of the uncomplexed form and the observed fluorescence decay was found to be mono-exponential. For the 1:1 complexes between Eu^{3+} or Fe^{3+} and PY a fluorescence decay time of ~ 1 ns was determined, which corresponds quite well to the short-wavelength component of the uncomplexed PY. Because of the very low fluorescence intensity of the 1:1 Me^{3+}-PY complexes the fit quality is poor and it is attractive to assume that the observed residual fluorescence is connected to a very small portion of uncomplexed PY still present in solution rather than to connect it to the Me^{3+}-PY complex.

In contrast, in the presence of Al^{3+} the fluorescence of PY was not quenched, however the overall fluorescence maximum was slightly shifted towards longer wavelengths. In addition, also the decay kinetics changed. At a ratio of 1:1 between PY and Al^{3+} a pure mono-exponential decay behaviour was observed. The fluorescence decay time for the 1:1 complex of Al^{3+} and PY was determined to be 4.1 ns and was independent of the detection wavelength used which is in contrast to the free PY or its complexes with other metal ions investigated.

From the results of the time-resolved measurements it can be concluded that a static fluorescence quenching is operating upon complexation of PY by Me^{3+}. The decrease of the steady-state fluorescence intensity was evaluated according to the Stern-Volmer formalism for the emission wavelength range between $350\,\text{nm} < \lambda_{em} < 375\,\text{nm}$ and $400\,\text{nm}\ \lambda_{em} < 425\,\text{nm}$, respectively. For both wavelength ranges the same K_{SV} was obtained. A value of $K_{SV} = (1.7 \pm 0.1) \cdot 10^6\ \text{M}^{-1}$ was calculated. Only in case of 1:1 complex K_{SV} can be used to directly derive a conditional binding constant. However, from spectrophotometric titration measurements according to Job's method, a complex stoichiometry of $\approx 2{:}3$ was determined (Hill and MacCarthy, 1986; Ledyard and Butler, 1997). This means, that the K_{SV} can not be referred to as the real binding constant. In comparison to other compounds, such as pyochelin, the binding strength seems to be in the same order of magnitude. For pyochelin in a 2:1 complex with Fe^{3+} in ethanol a binding constant of $2 \cdot 10^5\ \text{M}^{-1}$ has been determined (Namiranian *et al.*, 1997).

PY shows a complex photophysical behavior depending on the solvent. It is attractive to attribute the observed characteristics to intramolecular and solvent-assisted proton transfer reactions in the excited state. The excited state(s) (A*, B*) can be described by a double-well potential (Fig. 6). The form A* represents the excited state before and the form B* accounts for the excited state of the molecule after the proton transfer reaction.

In solvents with weak H-donating or -accepting properties like methanol an intramolecular reaction is dominant. After PY is photoexcited the

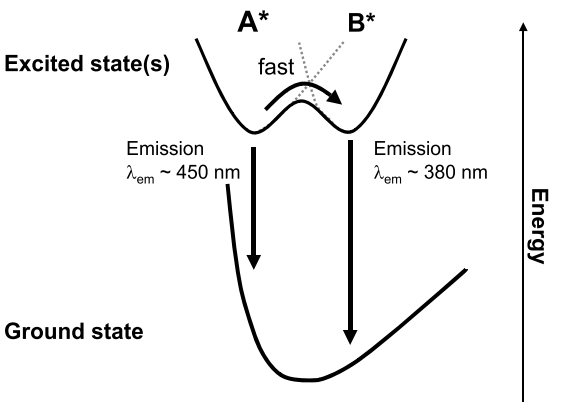

Fig. 6. PY relaxes to a state (A*) after photoexcitation. A* can show direct emission ($\lambda_{em} \sim 450$ nm). In a very fast reaction in the electronically excited state and in competition with the direct fluorescence from A*, B* can be formed. In case of MeOH as a solvent, a possible excited state reaction could be the breaking of an intramolecular H-bond of PY. Subsequently, B* itself can show fluorescence ($\lambda_{em} \sim 380$ nm).

electron distributions and the acidity of groups like -OH or -CONHR is altered. In particular the effect of photoexcitation on the electronic properties of the -CONHR-group seems to be important for the observed fluorescence characteristics. The electron accepting character of the -CONHR-groups of PY is reduced in the excited state and therefore, the acidity of the groups is decreased as well. This causes a break of the intramolecular H-bond between the amide and pyridine moiety of the molecule (see Fig. 6). Subsequently, the charge distribution in the molecule is changed and also the stabilization of the excited molecule by the solvent is altered, which leads to the observed blue shift of the emission (see Fig. 4).

On the other hand, in strong protic solvents like water a solvent-assisted proton transfer reaction is dominating the fluorescence of PY and now the phenolic groups of PY come into play. No intramolecular H-bond can be formed in aqueous solutions. The intramolecular H-bond between the amide and the pyridine moieties is blocked by water molecules. The observed trends in the absorption and fluorescence spectra at different pH values resemble the well-known pH behavior of benzoic hydroxy compounds. At low pH values the -OH-groups are protonated and the fluorescence is weak, while at $pH > 4$ a deprotonation of the -OH-groups leads to an increase of the fluorescence. Here, the observed spectral shift and the complex fluorescence decay can be attributed to solvent-assisted proton transfer reactions.

Except for Al^{3+}, the metal ions investigated quenched the fluorescence of pyridinochelin upon complexation. Al^{3+} did not quench the fluorescence but did change the fluorescence decay kinetics. Since Al^{3+} shows no heavy atom effect the fluorescence intensity stays unquenched. In the complexation process Al^{3+} competes successfully with H^+ for the binding sites, especially of the -OH-group and the amide group and eliminates upon binding the formation of inter- or intramolecular H-bonds with those groups. In addition the conformation of PY is fixed by Me^{3+} and twists around bonds, which could occur upon photoexcitation and which would also affect the fluorescence characteristics, are no longer possible. This is reflected in the observed alteration of the fluorescence decay and spectra – especially in the case of Al^{3+}. In the presence of Al^{3+} the fluorescence decay is mono-exponential which indicates that only one fluorescing species is present. This further supports the proposed two forms of PY that are formed in the excited state (see Fig. 6).

In our study the photophysics of PY was analyzed and it could be shown that the fluorescence properties are determined by ionic and non-ionic species that are formed upon photoexcitation. The extent to which each species contributes to the observed fluorescence is dependent on solvent conditions (*e.g.*, pH value) and the presence of metal ions. Consequently, the intrinsic fluorescence of PY can be used as a molecular probe for identification purposes, *e.g.*, to monitor the transport of iron by microorganisms.

Acknowledgements

The authors wish to thank S. Eidner (University of Potsdam) for performing the factor analysis of the absorption spectra as well as Noreen Splies and Stefanie Zilm (University of Potsdam) for the UV/Vis absorption measurements. The help of Ruediger Schnurre (TFH Berlin) for the synthesis of PY is gratefully acknowledged. Further, gratefully acknowledged is the financial funding by the Deutsche Forschungsgemeinschaft (LO 395/16-2).

Adolphs M., Taraz K., and Budzikiewicz H. (1996), Catecholate siderophores from *Chryseomonas luteola*. Z. Naturforsch. **51c**, 281–285.

Albrecht-Gary A. M., Libman J., and Shanzer A. (1996), Biomimetic Fe^{3+} trishydroxamate complexes and triple stranded diferric helices. Pure Appl. Chem. **68**, 1243–1247.

Barelmann I., Meyer J.-M., Taraz K., and Budzikiewicz H. (1996), Cepaciachelin, a new catecholate siderophore from *Burholderia (Pseudomonas) cepacia*. Z. Naturforsch. **51c**, 627–630.

Berlmann I. B. (1971), Handbook of Fluorescence Spectra of Aromatic Molecules, 2nd ed. Academic Press, New York.

Bodenant B. and Fages F. (1995), Synthesis, metal binding, and fluorescence studies of a pyrene-tethered hydroxamic acid ligand. Tetrahedron Lett. **36**, 1451–1454.

Budzikiewicz H. (1997), Siderophores of fluorescent *Pseudomonas*. Z. Naturforsch. **52c**, 713–720.

Budzikiewicz H. (2004), Bacterial catecholate siderophores. Mini-Rev. Org. Chem. **1**, 163–168.

Bultreys A., Gheysen I., Walthelet B., Schaefer M., and Budzikiewicz H. (2004), The pyoverdins of *Pseudomonas syringae* and *Pseudomonas cichorii*. Z. Naturforsch. **59c**, 613–618.

del Olmo A., Caramelo C., and SanJose C. (2003), Fluorescent complex of pyoverdin with aluminum. J. Inorg. Biochem. **97**, 384–387.

Ecker D. J., Loomis L. D., Cass M. E., and Raymond K. N. (1988), Substituted complexes of enterobactin and synthetic analogues as probes of the ferric-enterobactin receptor in *Escherichia coli*. J. Am. Chem. Soc. **110**, 2457–2464.

Fages F. (1997), Fluorescent, siderophore-based hydroxamate chelators for the detection of transition-metal ions. In: Chemosensors of Ion and Molecule Recognition, Vol. 492 (Desvergne J. P. and Czarnik A. W., eds.). Kluver Academic Publishers, Dordrecht, pp. 221–240.

Hill Z. D. and MacCarthy P. (1986), Novel approach to job's method. J. Chem. Educ. **63**, 162–167.

Ledyard K. M. and Butler A. (1997), Structure of putrebactin, a new dihydroxamate siderophore produced by *Shewanella putrefaciens*. J. Biol. Inorg. Chem. **2**, 93–97.

Meyer M. and Trowitzsch-Kienast W. (1997), Computational study of novel catechol-type siderophore analogs. J. Mol. Struc. **418**, 93–98.

Meyer M. and Trowitzsch-Kienast W. (2004), Theoretical and experimental studies of siderophore structure and function. Recent Res. Devel. Phys. Chem. **7**, 127–149.

Meyer M., Schnurre R., Reissbrodt R., and Trowitzsch-Kienast W. (2001), Computer-aided design of novel siderophores: Pyridinochelin. Z. Naturforsch. **56c**, 540–546.

Namiranian S., Richardson D. J., Russel D. A., and Sodeau J. R. (1997), Excited state properties of siderophore pyochelin and its complex with zinc ions. Photochem. Photobiol. **65**, 777–782.

Planche T., Marmolle F., Abdallah M. A., Shanzer A., and Albrecht-Gary A.-M. (1999), Fluorescent siderophore-based chemosensors: Fe^{3+} quantitative determinations. J. Biol. Inorg. Chem. **4**, 188–198.

Ruangviriyachai C., Fernandez D. U., Schaefer M., and Budzikiewicz H. (2004), Structure proposal for a new pyoverdin from a Thai *Pseudomonas putida* strain. Spectroscopy **18**, 453–458.

Rubini P., Lakatos A., Champmartin D., and Kiss T. (2002), Speciation and structural aspects of interactions of Al(III) with small biomolecules. Coord. Chem. Rev. **228**, 137–152.

Santos M. A. (2002), Hydroxypyridinone complexes with aluminium-*in vitro/vivo* studies and perspectives. Coord. Chem. Rev. **228**, 187–203.

Sohna J.-E. and Fages F. (1997), Sensitized luminescence of the europium(III) ion bond to a pyrene-containing triacid ligand. Tetrahedron Lett. **38**, 1381–1384.

Tor Y., Libman J., Shanzer A., Felder C. E., and Lifson S. (1992), Chiral siderophore analogs: Enterobactin. J. Am. Chem. Soc. **114**, 6661–6671.